Cell Communication and Signaling

RESEARCH

Open Access

The SHH/GLI target Netrin-1 supports self-renewal in medulloblastoma tumor cells

P. Falcón-Urrutia[1†], E. Fernández-Caniulén[1,2†], J. M. Zúñiga-Hernández[1], B. Gaete-Ramírez[3], C.P. Prieto[1], S. M. Pfister[4,5,6], M. Kool[4,5,7,8], U. Schüller[9,10,11], B. Wainwright[12], M. Remke[13], M.D. Taylor[14], F. Alvarez-Astudillo[3], R. Armisén[15], M. Varas-Godoy[3,16*] and V. Palma[1*]

Abstract

Deregulation of the Sonic Hedgehog (SHH)/GLI signaling pathway has been strongly implicated in carcinogenesis, particularly in brain and skin tumors, through mutations affecting various pathway components. Given its central role in tumor development, the SHH/GLI axis has emerged as a key target for therapeutic intervention, underscoring the need to identify GLI-specific targets in cancer cells. Netrin-1, a multifunctional signaling molecule with pro-oncogenic properties, is overexpressed in diverse tumor types. While its tumor-promoting functions are well documented, the regulatory mechanisms governing its expression remain poorly understood. Here, we provide through gene expression profiling and in vitro and ex vivo analyses evidence demonstrating that Netrin-1 (*NTN1*) is a direct transcriptional target of canonical SHH signaling. We further show that in conditions of SHH pathway hyperactivation—such as in SHH-driven medulloblastoma (MB) *NTN1* is significantly upregulated. This overexpression promotes the self-renewal of MB stem-like cells through the modulation of ERK signaling, thereby contributing to enhanced cancer stemness. Our findings identify *NTN1* as a novel downstream effector of the SHH/GLI pathway and demonstrate that quantifying *NTN1* levels can refine molecular classification of SHH-subtype medulloblastomas—distinguishing tumors with high SHH pathway activation and enhanced stem-like properties, with potential implications for prognosis and targeted therapy selection.

Keywords Netrin-1, Medulloblastoma, Sonic Hedgehog, Self-renewal, GLI, Cancer

Introduction

Sonic Hedgehog (SHH) signaling is one of the key pathways governing vertebrate development, regulating a wide range of processes, including stem cell niche establishment and organogenesis [1–4]. In the Central Nervous System (CNS), SHH is the only Hedgehog member expressed, acting as a potent morphogen during neural tube patterning, and playing a mitogenic role in dorsal brain expansion [5–8]. Specifically, SHH serves as the main mitogenic signal during postnatal cerebellum growth, targeting granular neural progenitors (GNPs). These GNPs actively proliferate in the external granular layer (EGL), a temporary germinative neuroepithelium located at the subpial surface of the developing

†P. Falcón-Urrutia and E. Fernández-Caniulén contributed equally to this work.

*Correspondence:
M. Varas-Godoy
manuel.varas@uss.cl
V. Palma
vpalma@uchile.cl

Full list of author information is available at the end of the article

© The Author(s) 2026. **Open Access** This article is licensed under a Creative Commons Attribution-NonCommercial-NoDerivatives 4.0 International License, which permits any non-commercial use, sharing, distribution and reproduction in any medium or format, as long as you give appropriate credit to the original author(s) and the source, provide a link to the Creative Commons licence, and indicate if you modified the licensed material. You do not have permission under this licence to share adapted material derived from this article or parts of it. The images or other third party material in this article are included in the article's Creative Commons licence, unless indicated otherwise in a credit line to the material. If material is not included in the article's Creative Commons licence and your intended use is not permitted by statutory regulation or exceeds the permitted use, you will need to obtain permission directly from the copyright holder. To view a copy of this licence, visit http://creativecommons.org/licenses/by-nc-nd/4.0/.

cerebellum [9, 10]. Once GNPs become unresponsive to SHH, they exit the cell cycle and migrate inward, guided by Bergman glial filaments, to form the internal granule layer, their final destination [2].

Growth factors that regulate the proliferation and maintenance of stem cells and progenitors are critical for maintaining a homeostatic proliferative balance. When this balance is disrupted, it can lead to malignancy. Aberrant activation of the SHH pathway has been linked to the induction of a cancer stem/progenitor cell phenotype. For example, persistent activation of the canonical SHH pathway in GNPs results in the development of SHH-driven medulloblastoma (MB), the most common pediatric primary CNS tumor [11–13]. SHH-subtype MB accounts for around 30% of all MB cases and has a bimodal incidence, predominantly affecting infants (< 3 years) and adults (> 16 years), while contributing less to childhood tumors (4–15 years) [14]. Clinically, SHH MB exhibits several histological phenotypes, with the desmoplastic/nodular subtype being the most representative. While most of the patients with SHH MB have relatively good outcomes, the toxicity of post-surgical treatments for MB, especially conventional radiotherapy, can lead to severe side effects, such as an IQ decrease when 36 Gy of craniospinal irradiation (CSI) is administered [15]. Therefore, there is a pressing need for new, targeted therapies that not only improve the survival rate but also enhance the life quality for affected patients [16].

Activation of the canonical SHH pathway begins when the SHH ligand binds to its transmembrane receptor PATCHED1 (*PTCH1*), relieving its inhibitory effect on the co-receptor SMOOTHENED (*SMO*). This triggers an intracellular cascade that culminates in the transcriptional regulation of target genes via the glioma-associated oncogene (GLI) downstream effectors. The GLI family (*GLI1*-3) comprises zinc-finger transcriptional factors that can either activate or repress target genes depending on the signaling context, with *GLI1* uniquely acting as a transcriptional activator, amplifying pathway activity [17]. GLI proteins bind to the consensus 9-mer DNA sequence –GACCACCCA- in the regulatory regions of their target genes, though variants with lower affinity but significant transcriptional activation have also been reported [18]. SHH/GLI signaling involves feed-forward and feedback loops, such as *GLI1* regulating *PTCH1* and auto-regulating its own expression. Activator forms *GLI2* and *GLI3* drive *GLI1* transcription, initiating a feed-forward loop in which *GLI1* amplifies its own expression. The importance of the so-called GLI code- the combinatorial action of *GLI1*-3 - is underscored by genetic or epigenetic changes that lead to aberrant activation of GLI, driving oncogenesis [19]. A genome-wide survey of *GLI1* GLI-binding sites (GBS) revealed numerous locations in both normal and malignant tissues. However, the expression patterns differed significantly between normal and tumor cells [20].

Given the broad biological significance of the SHH pathway in development and disease, identifying novel GLI targets is crucial for understanding how this pathway integrates its effects through fine-tuned mechanisms. This is especially relevant in cancer, where targeting specific signaling pathways for drug therapy is taking center stage, making the identification of GLI-specific targets in tumor cells essential.

Netrin-1 (encoded by *NTN1*) is the most well-characterized member of the laminin-related glycoprotein Netrin family, which includes Netrins 1–4 [21]. First discovered in a *C. elegans* screening (ortholog Unc-6) [22, 23], Netrin-1 was initially identified as an axonal guidance protein [24, 25]. However, it has been implicated in a wide range of cellular processes, including acting as a survival factor via interactions with the DCC/NEOGENIN1 (NEO-1) and UNC5s dependence receptor families, which trigger apoptosis in the absence of their ligands [26]. Netrin-1 also plays roles in cell survival [27], angiogenesis [28], cell adhesion [29], migration [30], and immune modulation [31–33].

Beyond its physiological roles, Netrin-1 is overexpressed in several cancers, including glioblastoma [34], neuroblastoma [26], MB [35], breast cancer [36], and gastric cancer [37]. In these contexts, Netrin-1 acts as a survival factor, inhibiting the apoptotic signaling generated by its receptors via autocrine secretion [38], and promoting cell migration [39] and invasion [40]. Delloye-Bourgeois et al. reported a truncated intranuclear form of Netrin-1(ΔN-Netrin-1), lacking the first part of the N-terminal domain IV, which stimulates cell proliferation by interacting with nucleolar proteins and ribosomal DNA promoters [41]. The ΔN-Netrin-1 truncated isoform promoter was found to be NF-κB dependent. Consequently, in cancers like pancreatic adenocarcinoma, gastric cancer, ovarian cancer, and brain metastases, the overexpression of Netrin-1 and ΔN-Netrin-1 has been associated with a poor prognosis [42–47].

Recent research highlights a new role for Netrin-1 in maintaining stemness in both development and cancer contexts [48–52]. Netrin-1 modulates cancer cell plasticity [49] and promotes stemness characteristics [34]. In glioblastoma, where cancer stem cells are well-characterized [53], Netrin-1 induces stemness via Notch pathway activation [34]. Blocking Netrin-1 in glioblastoma stem cells inhibits tumor growth, invasion, and angiogenesis [51].

Given the diverse biological roles of Netrin-1 across contexts, it is important to understand the mechanisms that regulate its expression. Although Netrin-1 is known as a transcriptional target of the NF-κB pathway [54], the developmental signaling that controls Netrin-1

expression remains unclear. However, there is consistent evidence that Netrin-1 is a direct transcriptional target of the SHH pathway. Netrin-1 is expressed in areas under strong SHH morphogenetic signaling, such as the neural tube floor plate [55]. Furthermore, *Netrin-1* in the ventral most of the spinal cord is lost in the *Gli2* mutant mice [56]. Netrin-1, like SHH, has also been reported in neurogenic niches in vivo in both embryonic and adult neural stem and progenitor cells [57]. In the postnatal cerebellum, Netrin-1 is strongly expressed in the EGL from P0 until P10, during murine development [58]. By performing global profiling of gene expression in different SHH/Gli gain- and loss-of-function scenarios and others, we established the Netrin-1 homolog *ntn1a* as a potential new SHH target in zebrafish [59, 60]. Also, Podjaski et al. demonstrated that modulation of the canonical SHH pathway induces *NTN1* up-regulation in human brain-derived endothelial cells [61].

Here, we demonstrate through gene expression profiling and in vitro and ex vivo functional analyses that Netrin-1 is a direct transcriptional target of the SHH/GLI pathway. Furthermore, we provide evidence that Netrin-1 supports the self-renewal of MB stem-like cells in DAOY, a widely used in vitro model of SHH-driven medulloblastoma, supporting its potential role in desmoplastic SHH-MB. Since MB consists mainly of undifferentiated stem- or progenitor-like cells, our findings offer new insights into therapeutic targeting for SHH-driven desmoplastic MB by interfering with Netrin-1.

Materials and methods

Gene expression profiling studies

MB and healthy brain expression data correspond to a compilation of 23 transcriptomic datasets reported under the GEO accession number GSE124814 and published in [62]. The data were analyzed and obtained through the genomics analysis and visualization platform R2 (https://hgserver1.amc.nl/).

In silico analysis

GLI1 binding sites in Netrin-1 gene elements: *GLI1*, *GLI2* and *GLI3*- DNA binding site consensus sequences were retrieved from HOCOMOCO v11 database. To scan TF binding sites, the *NTN1* gene promoter sequence elements were recovered from Ensembl (Human genome version GRCh38). The scanning was performed using FIMO (Find Individual Motif Occurrences) tool using the default background model [63].

Human medulloblastoma samples

The samples were obtained through collaborations with the German Cancer Research Center (Heidelberg, Germany), the Center for Neuropathology, Ludwig-Maximilians University (Munich, Germany), and the Hospital for Sick Children and the Brain Tumor Research Centre (Toronto, Canada). These samples had been molecularly characterized by neuropathologists in the respective histopathology core laboratories, following standard histology and Hematoxylin and Eosin (H&E) staining procedures (Supplementary Table 1). In compliance with internal regulations and national guidelines, all protocols were approved by the Bioethics Committees of the respective institutions (Certificate #1764-FCS-UCH), including the Faculty of Sciences and the Faculty of Medicine of the University of Chile and the Bioethics Committee of the National Fund for Science and Technology (FONDECYT, ANID).

Mouse models

All the experimental procedures involving the use of mice were approved and followed the guidelines of the University of Chile Ethics Committee (Certificate #1764-FCS-UCH).

GNP cell isolation

Primary GNP cultures were prepared from the postnatal cerebellum (P6) of mice according to the procedures described in [9].

Immunostaining

Samples were deparaffinated by incubation at 60 °C for one hour, followed by washing in xylol, and rehydration through a graded series of ethanol solutions. After rehydration, immunohistochemistry was performed on tissue sections according to established protocols [64]. The following antibodies were used: anti-Netrin-1 1/400 (#H-104, Santa Cruz), anti-β-III tubulin 1/1000 (#T8660, Sigma), anti-PCNA 1/100 (#13-3900, Invitrogen), anti-Sox2 1/200 (#ab97959, ABCAM) and TOPRO 1/200 (#T3605, Invitrogen). Standard optimized procedures were applied to enhance antigen retrieval, primary antibody dilution, and other relevant factors. Stained sections were dehydrated in xylol and mounted with Entellan. Confocal imaging was conducted using a Zeiss LSM 510 META, and fluorescence microscopy was performed with an Olympus BX-51 microscope.

Cell culture

The DAOY human medulloblastoma cell line (#HTB-186, ATCC), which is predicted to be the SHH subtype, was cultured in high glucose Dulbecco's Modified Eagle Medium (DMEM, Gibco) supplemented with 10% fetal bovine serum (FBS, Hyclone), penicillin 10,000 U/mL and 10,000 µg/mL streptomycin. HEK293T cells were cultured in DMEM containing 10% FBS, 10,000 U/mL penicillin, and 10,000 µg/mL streptomycin, following standard procedures [35].

ChIP, chromatin immunoprecipitation

The ChIP assay was performed as described by Soutoglou & Talianidis [71], with minor modifications. Nuclear extracts were obtained by sonication of DAOY cells, producing chromatin fragments between 200 and 500 bp. For each immunoprecipitation, 25 µg of sheared chromatin was incubated with 5 µg of antibody against *GLI1* (# NB600-600, Novus Biologicals), *GLI2* (# ab26056, ABCAM) or GLI3 (# H-280, Santa Cruz). A histone H3 antibody (#ab1791, ABCAM) served as a positive control, whereas normal Rabbit IgG (#sc-2027, Santa Cruz) was used as the negative immunoprecipitation control. DNA recovered from the immune complexes was quantified by SYBR Green qPCR, using 1µL of the INPUT and 5µL of each IP sample. The reaction parameters were set using an INPUT concentration curve. An independent positive-control ChIP targeting the human *PTCH1* promoter verified assay performance.

Luciferase assay

The transcriptional contribution of the proximal *NTN1* promoter (–2 kb upstream of the transcription-start site) was analyzed in DAOY medulloblastoma cells using a dual-luciferase system. The – 2 kb fragment containing the wild-type GLI-binding site 1 (GBS1) was PCR-amplified and inserted upstream of the Firefly Luciferase gene in pGL3-Basic. A derivative construct in which the core GBS1 motif was mutated (hereafter Mut GBS1) was generated by site-directed mutagenesis to abolish GLI binding. DAOY cells (1 × 10^5 cells per well, 12-well plates) were transfected with Lipofectamine Plus (Invitrogen) according to the manufacturer's instructions. For transactivation assays with the wild-type reporter, cells were co-transfected with 500 ng of *NTN1*-Luc reporter, 50 ng of the pRL-TK Renilla plasmid (internal control), and either 150 or 300 ng of *GLI1* or GLI3A expression plasmids, or an empty vector (control). For mutation analysis, only *GLI1* (300 ng) was co-transfected with either the wild-type or Mut GBS1 reporter.

After 3–5 h in serum-free medium, cells were returned to complete growth medium, incubated for 48 h and harvested. Lysates were prepared with Passive Lysis Buffer (Promega), and Firefly and Renilla activities were quantified sequentially using the Dual-Luciferase® Reporter Assay System (E1960, Promega) on an Infinite® M1000 Pro plate reader (Tecan). Relative luciferase units (RLU) were calculated as the Firefly/Renilla ratio and normalized to the empty-vector control.

As a positive control for GLI-mediated transcription, cells were co-transfected with *GLI1* and GLI3A along with a GLI-responsive luciferase plasmid containing eight tandem GLI-binding sites (8xGBS-Luc; GBS, specific GLI Binding Site) [65].

RNA extraction and reverse transcription

Total RNA was extracted in a single step using the TRIzol™ reagent (Invitrogen) and stored at -80 °C until further processing. Total RNA (1 µg) was reverse transcribed using the iScript ™ cDNA Synthesis kit (BioRad), following the manufacturer's instructions.

SYBR green real-time qPCR assays

Real-Time qPCR was performed using the Brilliant II SYBR® Green QPCR Master Mix kit and the Stratagene Mx3000P real-time PCR system (Agilent Technologies). Data analysis was conducted using MxPro Software, with relative quantification determined by the comparative Ct method using β-actin as the internal parameter. Genes and primers are detailed in Supplementary Table 2.

Recombinant SHH treatment

DAOY cells or GNPs were seeded in 6-well plates at a density of 50,000 cells per well. After 24 h, the medium was replaced with EMEM containing 0.5% fetal bovine serum (FBS) and treated with either 0.1% BSA (vehicle control) or 20 nM recombinant SHH (R&D). After the treatment period (24–48 h), the cells were washed with PBS 1X, trypsinized, and trypsinization was halted by adding two volumes of complete medium. The cells were then centrifuged to obtain a pellet, which was either stored at -20 °C or processed for protein or RNA extraction.

Quantitative PCR based on Taqman probes

The reaction was carried out with specific primers in a LightCycler 480 apparatus (Roche) using the LightCycler TaqMan Master Kit (Roche) following the manufacturer"s instructions. In the case of human samples such as DAOY cells, the normalization control was *β-actin*, whereas for murine samples such as GNP cells, the normalization control was *Hprt*. Fluorescence was measured using LightCycler 4.05 software. The Ct values for each point were obtained both for the normalizing gene and the genes evaluated in each experiment. The amount of target transcripts, normalized against the housekeeping gene, was calculated using the comparative Ct method [61]. The genes and Taqman primers are detailed in Supplementary Table 3.

Western blot

For Western blot analysis, 40–70 µg of total proteins was loaded and separated on a 10% SDS-PAGE system. Proteins were transferred to 0.45 µm nitrocellulose membranes using the Transblot semi-dry transfer system (Biorad). Blocking was performed with 5% skim milk in TBS for 1 h, followed by incubation with the primary antibodies at 4 ° C for 1 h. After three washes with TBS-Tween, the membrane was incubated with the

corresponding secondary antibody for 3 h. The membrane was washed three times for 10 min and revealed with the chemiluminescent reagent (Pierce) using the SYNGENE G: BOX equipment (Synoptics Ltd). Primary antibodies used were anti-NTN-1 1/400 (# AF6419, R&D), anti-*SOX2* 1/200 (#ab97959, ABCAM), anti-β-actin 1/1000 (#A5316, Sigma-Aldrich), anti-ERK1/2 1/1000 (#4695, Cell Signaling), anti-p-ERK1/2 1/1000 (#4370, Cell Signaling). The secondary antibodies used were anti-sheep HRP 1/1000 (#HAF016, R&D), anti-mouse HRP 1/2000 (#7076, Cell Signaling), and anti-rabbit HRP 1/1000 (#7074, Cell Signaling). Quantifications were performed using integrated density analysis with ImageJ software (National Institutes of Health, USA).

Lentiviral transduction and stable Netrin-1 knockdown cell line generation

To generate a stable Netrin-1 knockdown line, the CRISPRi plasmid pLVhU6-sgRNAhUbC-dCas9-KRAB-T2a-Puro (#71236, Addgene) was used. Guide RNAs targeting the *NTN1* promoter (sg1NTN1, sg2NTN1) and control guide (sgCTL) were designed using CHOP-CHOP and cloned into the plasmid. HEK293T cells were triple-transfected with psPAX2 (#12260, Addgene), pCMV-VSV-g (#8454, Addgene), and pLVhU6-sgRNA-hUbC-dCas9-KRAB-T2a-Puro using the CaCl2 transfection method [66]. Viral supernatants were collected 60 h post-transfection, centrifuged at 1000 rpm for 5 min, filtered through a 0.45 µm filter and applied in a 1:1 ratio of culture media to DAOY cells. Stable lines were selected with puromycin (2 µg/mL), and knockdown efficiency was evaluated by RT-qPCR, Western blot, and immunofluorescence.

Tumorsphere formation assay

DAOY sgCTL and sg2NTN1 cells, were cultured in DMEM/F12 medium supplemented with epidermal growth factor (EGF; Invitrogen; 20 ng/mL), basic fibroblast growth factor (bFGF; Gibco; 20 ng/mL), insulin (Sigma-Aldrich, St. Louis, MO, USA; 5 µg/mL) and B-27 Supplement (Gibco; 1X). Cells were seeded at 1×10^3 cells/mL in ultra-low attachment 96-well plates and cultured at 37 °C, 5% CO2. Cultured medium was added every other day. After 7 days, tumorsphere formation was imaged using a Zeiss Axiovert S100 phase-contrast microscope. Sphere number and size were quantified using Zen 3.2 and ImageJ software.

Tumorsphere formation was also assessed in sgCTL and sg2NTN1 DAOY cells supplemented with human recombinant Netrin-1 (6419-N1, R&D), added every other day at 200 ng/mL. Similarly, ERK inhibition was performed with the selective ATP-competitive ERK1/2 inhibitor LY3214996, MedChemExpress) at 1µM [67].

Flow cytometry analysis

DAOY cells (1×10^5) were cultured in 6-well plates and harvested 24 h later by trypsinization with Trypsin-EDTA (0.25%; Gibco). Cells were resuspended in PBS with 1% BSA and 1 mM EDTA and incubated with 5 µL of CD24-PE antibody (# 130-098-861, Miltenyi Biotec) for 30 min at room temperature in the dark. After washing, cells were analyzed on a FACS CantoII (Becton Dickinson). Doublets and dead cells were excluded by gating using FSC and SSC.

Statistical analysis

Data were analyzed using Prism 5 software. A Shapiro-Wilk normality test was performed to assess the data distribution. For non-parametric data, a Kruskal-Wallis test was used for groups larger than 8, and the Mann-Whitney test for smaller groups. Parametric data were analyzed by ANOVA.

Results

NTN1 overexpression in SHH-driven MB

MB has been classified into four molecular groups: WNT, SHH, Group 3, and Group 4, based on DNA methylation and/or transcriptional profiling, as established by an international panel of experts [68, 69]. In our study, we conducted extensive transcriptomic meta-analyses using a cohort of 291 normal cerebellum samples and 1213 human MB samples distributed across these four molecular groups: WNT (112), SHH (390), Group 3 (222), and Group 4 (489). Our analyses revealed elevated levels of transcriptional expression of *NTN1* in SHH-driven MBs compared to the normal cerebellum and MB Groups 3 and 4 (Fig. 1A, Supplementary Table 4). Interestingly, *NTN1* also showed high transcriptional levels in the WNT-MB subgroup. Additionally, we examined the expression profiles of the known SHH target genes, *GLI1* and *PTCH1*, both of which were overexpressed in the SHH-MB group (Fig. 1B and C, Supplementary Tables 5 and 6). These findings suggest that Netrin-1 is a potential SHH signaling target, with the possibility of defining a distinct *NTN1*-high subgroup within SHH-driven MB. Notably, this may intersect with SHH subtypes as defined by the WHO classification (e.g., *TP53*-mutant vs. *TP53*-wildtype), warranting further investigation.

Netrin-1 expression in MB tumor cells

Histologically, MB manifests in four variants: classic, anaplastic/ large cell, nodular /desmoplastic and MB with extensive nodularity [70]. The latter two are found exclusively in the SHH-driven MB, with nodular/desmoplastic being the most common within this group. This histological variant is characterized by neural differentiation within nodules (Fig. 1D, black asterisk), and active proliferation in the internodular zones (Fig. 1D, black arrow).

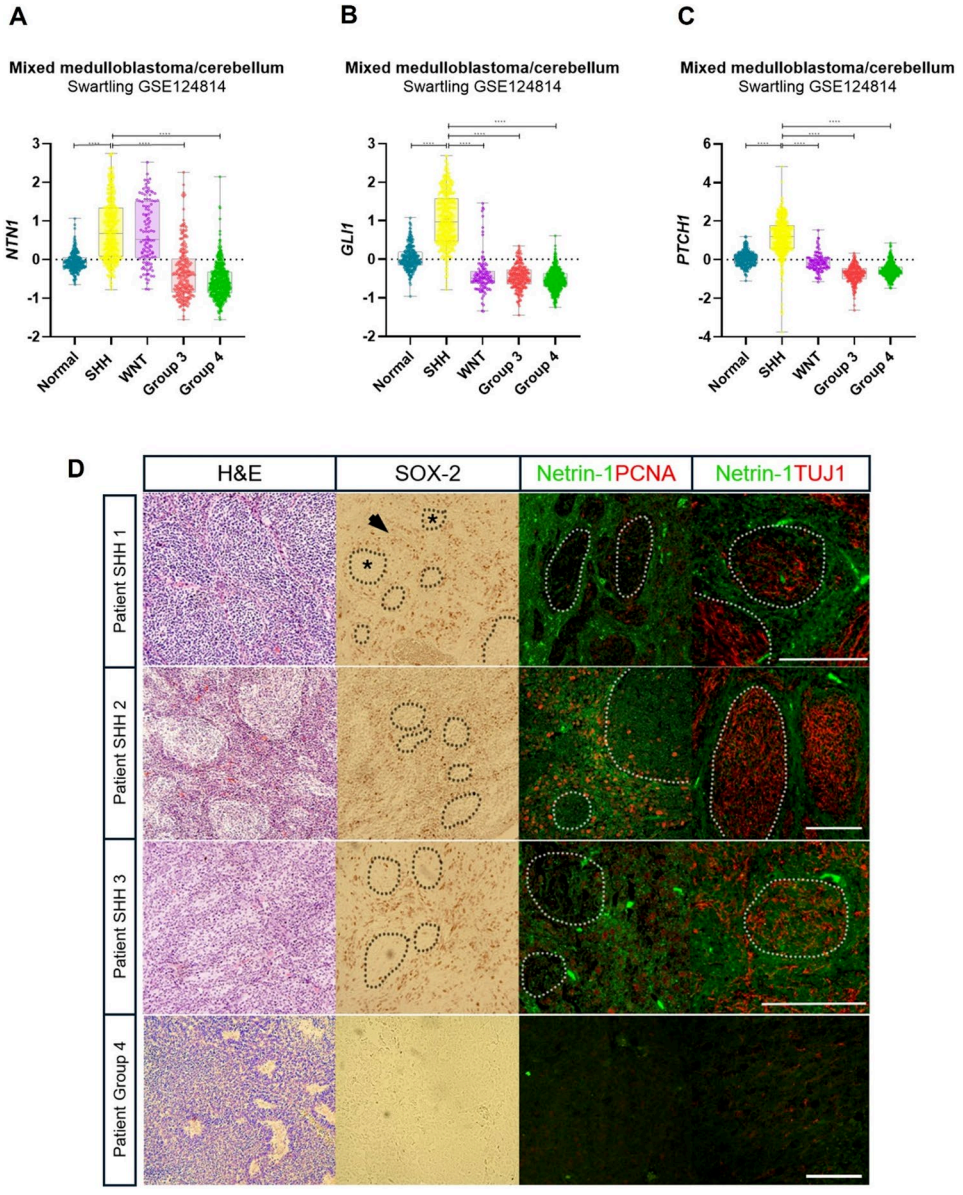


Fig. 1 Differential overexpression of Netrin-1 in SHH- driven MB tumor cells. Bioinformatic analysis of transcriptomic data from 291 normal cerebellum samples and 1,213 medulloblastoma (MB) samples revealed that *NTN1* is overexpressed in the SHH subgroup of MB (**A**). Similarly, classical targets of the SHH/GLI signaling pathway, including *GLI1* and *PTCH1*, are highly expressed in tumor samples from SHH MB (yellow circles), but are largely absent in normal cerebellum (blue circles) and in other MB subgroups (WNT: purple circles, Group 3: red circles, and Group 4: green circles). Statistical significance highlighted in the figure corresponds to one-way ANOVA with Welch's correction followed by Bonferroni-adjusted post hoc comparisons, indicating significant differences between the SHH subgroup and all other groups; detailed p-values for all pairwise group comparisons are provided in Supplementary Tables 4–6. (**B** and **C**). The desmoplastic histological variant is predominantly found in the SHH subgroup, characterized by nodules showing concentrated neuronal differentiation (black asterisk), while the internodular regions consist of highly proliferative tumor cells (black arrow). Netrin-1 expression is primarily observed in the internodular regions of SHH-driven MB, where tumor *SOX2*-positive cells proliferate in response to SHH/GLI signaling, as illustrated in a representative SHH sample. Consistent with Netrin-1 being active in proliferating tumor cells, the majority of Netrin-1 positive cells were indeed found co-localizing with PCNA, whereas no clear correlation with TUJ1, a neuronal cell differentiation marker, could be found. For comparison, a no-SHH MB sample from Group 4 is shown as a control. No evident pattern for Netrin-1 expression could be identified in this sample (**D**)

Consequently, we analyzed the expression and distribution of Netrin-1 protein across medulloblastoma molecular groups, comparing SHH with non-SHH tumors (WNT, Group 3, and Group 4). Immunostaining revealed that most Netrin-1-positive cells are present in these internodular zones (Supplementary Fig. S1 and Supplementary Table 7), colocalizing with the proliferation marker PCNA in proliferating tumor cells (Fig. 1D). Conversely, no significant correlation with the neural differentiation marker TUJ1 (β-III tubulin) was observed (Fig.

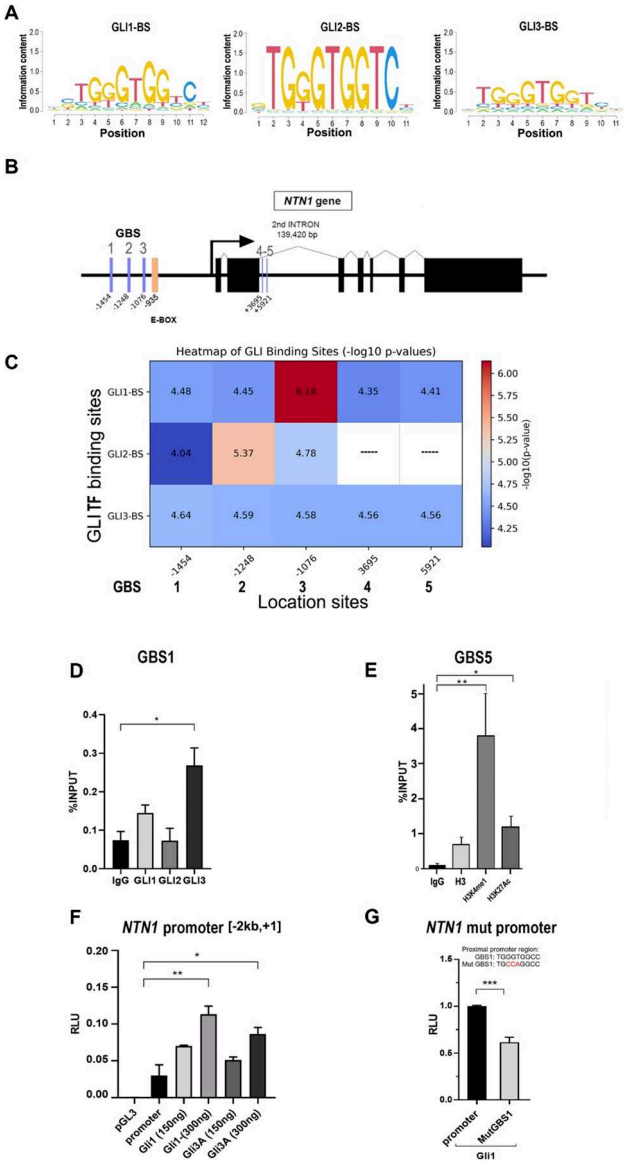


Fig. 2 GLI binding sites in *NTN1* regulatory regions are recognized by GLI transcription factors. **A** HOCOMOCO v11 (ChIP-seq) sequence logo generated from the position weight matrices (PWMs) of the three GLI transcription factors. **B** Schematic representation of the *NTN1* gene showing genomic regulatory elements and predicted GLI binding sites (GBSs), numbered above the map. **C** The heatmap depicts valid GBSs within the locus (X axis) with their best GLI match (Y axis) with their significance level in -log10(p-value) scale, where higher values indicate stronger significance. **D** ChIP-PCR analysis of GLI transcription factor binding at the promoter GBS1. **E** ChIP-PCR analysis of intronic GBS5 for histone H3 and its post-translational modifications, demonstrating a chromatin state permissive for active transcription at the GBS5 regulatory element. **F** Luciferase reporter assay using the cloned *NTN1* promoter region (− 2 kb to + 1 bp) to assess transcriptional activation in the presence of GLI factors. **G** Luciferase assay testing GBS1 binding activity using a mutated GBS1 site in the presence of *GLI1*. Statistical significance: $p < 0.05$ (*), $p < 0.01$ (**), $p < 0.001$(***)

1D). As a positive control of active SHH/GLI signaling, we analyzed the presence of SOX-2 [71], a cancer stem cell marker [72, 73]. Accordingly, SOX-2 distribution was predominantly localized in the internodular regions (Fig. 1D). This pattern further supports the expression of Netrin-1 in SHH-driven MB tumor cells, with no detectable Netrin-1 expression in non-SHH MB, as illustrated by a representative Group 4 MB sample (Fig. 1D).

Two intracellular Netrin-1 distribution patterns were noted in SHH- driven MB: nuclear-cytoplasmic and cytoplasmic (Supplementary Fig. S2). Interestingly, the nuclear-cytoplasmic pattern was also observed in the human MB cell line DAOY (Supplementary Fig. S3, see also Supplementary Fig. S4C), consistent with the presence of ΔN-Netrin-1. This isoform localizes to the nucleolus, where it interacts with nucleolar proteins and ribosomal DNA promoter sequences, promoting cell proliferation [41].

Taken together, our results indicate that Netrin-1 expression is predominantly associated with SHH-driven MB tumor cells, though low levels of expression were also observed in some WNT-MB tumors (data not shown).

GLI effectors bind to *NTN1* regulatory regions

To determine whether *NTN1* is a direct transcriptional target of the SHH/GLI pathway, we first performed an in-silico analysis using position weight matrices (PWMS) from the HOCOMOCO v11 database to identify putative GBSs within the *NTN1* promoter (Fig. 2A). This analysis revealed three candidate GBSs (GBS 1–3), located within a 2-kb proximal region upstream of the *NTN1* transcription start site (Fig. 2B). Interestingly, an E-box motif was also found in proximity to GBS1, suggesting potential regulatory crosstalk. Notably, the *NTN1* gene also contains putative GBSs in intronic regulatory element 2 (GBS 4 and 5), suggesting that SHH/GLI signaling may regulate *NTN1* transcription through this element (Fig. 2B Supplementary Table 8). To assess the statistical strength of these predicted GBSs, we generated a heatmap of $-\log_{10}$(p-values) corresponding to PWM matches across the promoter region. Among the three sites, GBS1 displayed the highest PWM score across *GLI1*, *GLI2*, and *GLI3* matrices, highlighting it as a strong candidate for functional GLI-mediated regulation (Fig. 2C). To experimentally validate GLI protein binding to GBS1, we conducted chromatin immunoprecipitation (ChIP) assays in DAOY medulloblastoma cells using antibodies against *GLI1*, *GLI2*, and *GLI3*. The canonical SHH target gene *PTCH1* was used as a positive control to confirm *GLI2* and *GLI3* binding (Supplementary Fig. S5A). Additional ChIP controls included IgG and histone H3 precipitations for both *PTCH1* and *NTN1* promoter regions (Supplementary Fig. S5B–C). At the *NTN1* promoter, significant enrichment of GLI3 was detected at the GBS1

site compared to the IgG control (Fig. 2D). On the other hand, immunoprecipitation with antibodies against either *GLI1* or *GLI2* did not show significant differences. Notably, the lack of endogenous *GLI1* enrichment at GBS1 does not rule out this site"s responsiveness to *GLI1*, as shown by the luciferase assays described below. Finally, given the intronic position of GBS5, we evaluated the possible role of this sequence as a transcriptional enhancer. For this purpose, we performed ChIP analysis using antibodies against post-translational modifications of histones associated with transcriptionally activated enhancers, such as H3K4Met1 and H3K27Ac. Interestingly, GBS5 was amplified when immunoprecipitating with both antibodies, revealing statistical significance compared to the IgG control (Fig. 2E).

GLI1 activates *NTN1* transcription through GBS1

To assess the functional significance of the identified GBS1 within the *NTN1* promoter, we performed dual-luciferase reporter assays in DAOY cells. A 2-kb fragment of the *NTN1* proximal promoter containing GBS1 was cloned upstream of the Firefly luciferase gene in the pGL3-Basic vector. A mutated version of GBS1 (Mut GBS1), in which the core GLI-binding motif was disrupted, was generated by site-directed mutagenesis. Each construct was co-transfected with a Renilla luciferase plasmid to control for transfection efficiency. Reporter assays were carried out in the presence of either *GLI1*, a potent transcriptional activator, or a constitutively active form of GLI3 (GLI3A). As a positive control for GLI-mediated transcription, a synthetic reporter containing eight tandem GLI-binding sites (8xGBS-Luc) was co-transfected with *GLI1* or GLI3A, resulting in robust luciferase activation (Supplementary Fig. S5D), confirming the activity of the GLI constructs. Co-transfection of the wild-type *NTN1* reporter with either *GLI1* or GLI3A resulted in dose-dependent increases in luciferase activity, with *GLI1* eliciting a significantly stronger transactivation compared to GLI3A (Fig. 2F). Importantly, mutation of GBS1 completely abolished *GLI1*-mediated transcriptional activation, demonstrating that this site is necessary for *NTN1* promoter responsiveness to *GLI1* (Fig. 2G).

Interestingly, sequence analysis revealed the presence of an E-box motif located at – 935 bp relative to the transcription start site, in close proximity to GBS1 (Fig. 2B). E-box motifs are typically recognized by basic helix-loop-helix (bHLH) transcription factors and have been shown to cooperate with SHH/GLI signaling components during oncogenic transformation of GNPs [20].

These results, in conjunction with our ChIP-qPCR data, provide functional evidence that *GLI1* directly engages GBS1 to activate *NTN1* transcription, and suggest a context-dependent interplay between *GLI1* and nearby E-box-binding factors in regulating *NTN1* expression.

NTN1 responds to SHH/GLI signaling modulation

We next assessed the impact of SHH/GLI pathway modulation on *NTN1* expression in DAOY cells. Treatment with recombinant SHH for 24 h induces a significant increase in *GLI1* and *NTN1* levels, compared to the control condition (Fig. 3A and B). These confirm that *NTN1* is a SHH/GLI transcriptional target, with implications for tumorigenesis when its signaling is dysregulated. Given that medulloblastoma is a neoplasia that originates from genetic abnormalities of the SHH pathway acting on cerebellar progenitors, we also sought to evaluate the SHH signaling regulatory role on mNetrin-1 expression in an ex vivo approach. In the extension of our study, 24 and 48-hour activation of the Shh/Gli pathway on wildtype (WT) mice GNP led to a significant increase in transcriptional levels of *mNetrin-1* and *mGli1* (Supplementary Fig. S6A and S6B).

Taken together in vitro and ex vivo data reported here support that Netrin-1 is a direct transcriptional target of SHH/GLI signaling in the context of cerebellar development as well as in cancer, suggesting that Netrin-1 signaling function and control play a pivotal role during the development, while altered might contribute to cell-death signaling dysregulation, consequently giving rise to neoplasia. Likewise, these pieces of evidence, both in mouse models and in human samples, suggest that signaling regulation is conserved between mammals.

Netrin-1 supports the self-renewal of MB stem-like cells

Given that Netrin-1 is expressed in proliferative, poorly differentiated areas of desmoplastic MB, we investigated its role in cancer stem cell maintenance. Using CRISPR interference (CRISPRi) to knockdown *NTN1* in DAOY cells, we verified the efficient downregulation of Netrin-1 (Fig. 4A, Supplementary Fig. S4). Even though two different sequences (sgRNAs) downregulated the Netrin-1 transcript (Supplementary Fig. S4A), only sg2NTN1 substantially diminishes the Netrin-1 protein expression (Supplementary Fig. S4B-C), and hence this cell line was selected for subsequent experiments. Under tumorsphere inducing culture conditions, we found a significant reduction in tumorsphere formation in the sg2NTN1 cell line (Fig. 4B). However, the diameter of the spheres generated from the Netrin-1 knockdown cells was similar to the spheres generated from the control. Through FACS, we observed a decrease in CD24-positive MB progenitor cells [74] in Netrin-1 knockdown cells relative to the control cell line (Fig. 4C).

Supplementation with exogenous recombinant Netrin-1 (200 ng/ml) was insufficient to rescue the phenotype (Fig. 4D). These findings suggest that Netrin-1

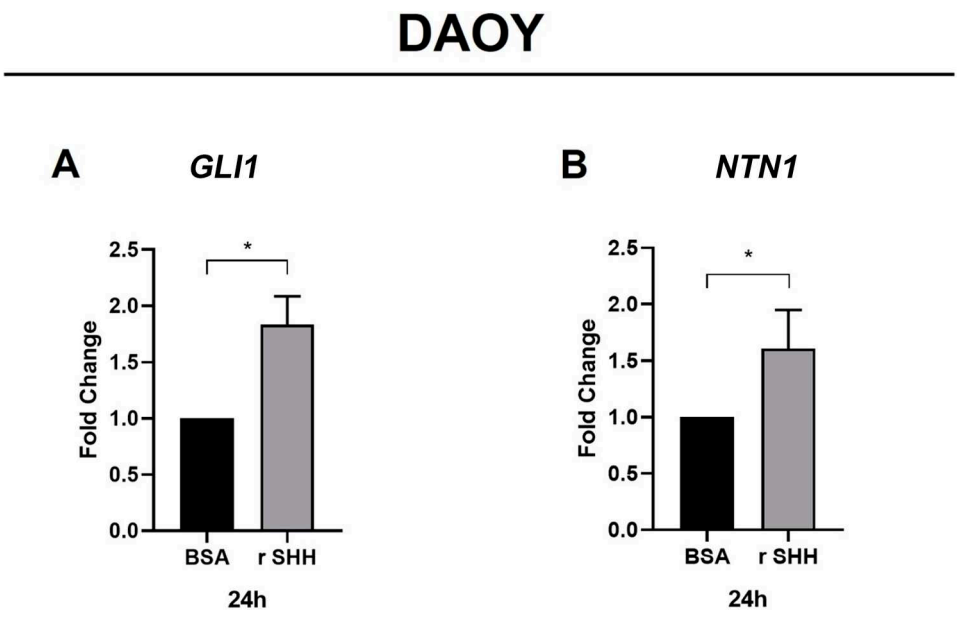


Fig. 3 *NTN1* transcriptional levels respond to SHH/GLI signaling modulation in vitro. The SHH/GLI pathway was activated in DAOY by treating them with 20nM recombinant SHH. After 24 hours of treatment, a significant increase in both transcriptional *GLI1* and *NTN1* levels was observed compared to the 0.1% BSA control (**A**, **B**). Error bars represent SEM; p values were calculated using the Mann-Whitney test from three independent experiments. Statistical significance is indicated as **P*<0.05

supports self-renewal of MB stem-like cells, without affecting their proliferation. Because an exclusively extracellular ligand failed to recover the knockdown phenotype, these data also strongly imply that MB stem-like self-renewal relies on the intracellular or intracrine functions of the Netrin-1 axis.

ERK signaling is involved in the effects of Netrin-1 on medulloblastoma stem-like cells

Interestingly, we verified that sg2NTN1 cells exhibit higher levels of ERK1/2 phosphorylation in comparison to the control (Fig. 4E and Supplementary Fig. S7). Netrin-1 was previously shown to maintain mESC self-renewal by activating the WNT pathway and inhibiting the MAPK pathway through ERK1/2 dephosphorylation/inactivation [48]. We therefore evaluated whether ERK1/2 activation was mechanistically involved in the reduced cancer-stem-cell population observed after Netrin-1 knockdown, treating both Netrin-1-knockdown and control DAOY cell lines with the MEK/ERK inhibitor LY3214996 (1 μM) every other day for one week. Inhibition of ERK recovered the significant reduction of tumorsphere formation observed in Netrin-1-knockdown DAOY cells (Fig. 4F), suggesting that Netrin-1 supports self-renewal of MB stem-like cells by modulating the MAPK pathway.

Taken together, our results demonstrate that Netrin-1 is a critical SHH/GLI target that promotes MB tumorigenesis by supporting the self-renewal of MB stem-like cells and modulating key developmental pathways. Thereby reinforcing the stem-like state and contributing to tumor persistence.

Discussion

Netrin-1 was originally identified as a key axonal guidance molecule [23]. However, the discovery that its receptor families also play roles in apoptosis modulation sparked a new research direction, focusing on Netrin-1's involvement in cell survival. This property has garnered significant interest in cancer research, given its potential to modulate pro-apoptotic receptor signaling [75]. Consequently, investigations have expanded to explore the pleiotropic functions of Netrin-1, driven by its diverse receptor repertoire.

In the context of cancer, NF-κB has been implicated as a regulator of Netrin-1 gene expression, with evidence also suggesting involvement of the tumor suppressor p53 [38, 54]. Nonetheless, the developmental signaling pathways controlling Netrin-1 expression have remained elusive. Here, we demonstrate that the canonical SHH/GLI signaling pathway directly regulates Netrin-1 expression at the transcriptional level, particularly in SHH-driven MB. Furthermore, these findings raise the possibility of a distinct *NTN1*-defined subgroup within SHH-driven MB. Future studies should investigate whether this subgroup aligns with SHH subtypes delineated by the WHO classification, such as *TP53*-wildtype and *TP53*-mutant variants.

A recent study by Podjaski et al. revealed that canonical SHH signaling regulates Netrin-1 expression in

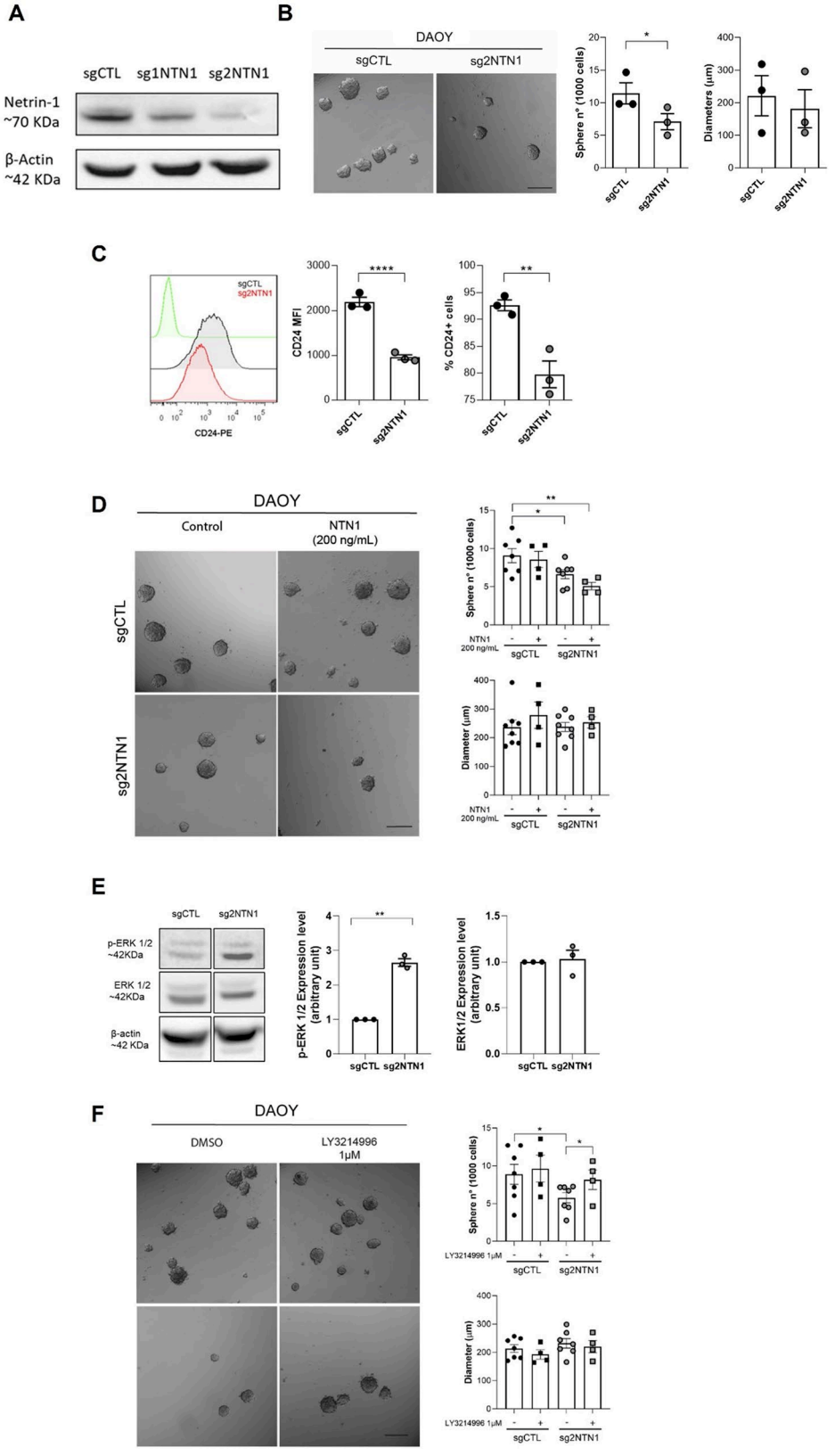


Fig. 4 (See legend on next page.)

(See figure on previous page.)

Fig. 4 Netrin-1 supports the self-renewal of DAOY stem-like cells. (**A**) Western blot analysis confirmed the successful lentiviral transduction of the CRISPRi system in DAOY, resulting in the downregulation in both sg1NTN1 and sg2NTN1 cells. (**B**) Tumorsphere derived from sgCTL and sg2NTN1 DAOY were imaged, analyzing sphere number and diameter. Tumorsphere formation analysis demonstrated a smaller number of spheres generated by sg2NTN1 cells relative to the control, indicating that Netrin-1 plays a role in supporting the cancer stem cell self-renewal capacity. Statistical analysis was performed using one-way ANOVA from three independent experiments, (mean ± SEM, $*p < 0.05$). (**C**) FACS analysis further revealed a reduced percentage of CD24 stem marker- positive cells in sg2NTN1 cells compared to the control. In the FACS histogram, the green curve represents autofluorescence of cells without the antibody, the black curve shows the fluorescence of sgCTL, and the red curve indicates the fluorescence in sg2NTN1. Statistical analysis was performed using one-way ANOVA from three independent experiments, (mean ± SEM, $**p < 0.01$, $****p \leq 0.0001$). (**D**) Tumorsphere formation was evaluated in DAOY sgCTL and sg2NTN1 cells exposed to recombinant human Netrin-1 (200 ng/mL). Representative images of the spheres obtained from each group are shown. Scale bar: 200 µm. Statistical analysis was performed using Shapiro–Wilk normality testing followed by Student's t-test from four independent experiments, (mean ± SEM, $*p < 0.05$, $**p < 0.01$). (**E**) Western blot analysis revealed elevated levels of phosphorylated ERK 1/2 in sg2NTN1 cells, suggesting that Netrin-1 maintains self-renewal partly through inhibition of the MAPK pathway. Densitometric analysis was performed to quantify protein levels, which were normalized to β-actin and expressed relative to the control condition (sgCTL = 1). Statistical analysis was performed using one-way ANOVA from three independent experiments, (mean ± SEM, $**p < 0.01$). (**F**) Tumorsphere formation was evaluated in cells exposed to the selective ERK1/2 inhibitor LY3214996 (1 µM). Representative images of the spheres obtained from each group are shown. Scale bar: 200 µm. Statistical analysis was performed using Shapiro–Wilk normality testing followed by Student's from four independent experiments t-test (mean ± SEM, $*p < 0.05$)

human brain-derived endothelial cells, with implications for autoimmune CNS diseases due to its anti-inflammatory effects [61]. Given the well-established connection between chronic inflammation and cancer, we sought to determine whether Netrin-1 is a downstream effector of SHH signaling in MB. Our data show that activation of the canonical SHH pathway directly regulates Netrin-1 acting through a functional GBS1 in the *NTN1* promoter region.

MB is the most common malignant pediatric brain tumor, yet despite extensive research into its molecular drivers, effective therapies remain elusive due to the tumor's heterogeneous nature. MB consists of distinct molecular groups, each with unique clinical and molecular characteristics, which lead to varying clinical outcomes [70, 76]. Over the past decade, research has focused on functionally validating genes and molecular processes that have been implicated in human genomic studies. Identifying molecular biomarkers for early diagnosis and treatment stratification across MB groups is crucial for improving therapeutic outcomes [77].

SHH-driven MB represents an intermediate prognosis group. Germline mutations in genes encoding negative regulators of the SHH pathway, such as *PTCH1* or suppressor of fused homologue (*SUFU*), lead to the development of SHH MB, as do somatic mutations and copy number alterations in pathway components, including in *GLI2* [77–79]. We and other groups have identified transcriptional targets active during embryonic development and in cancer [79, 80]. In the cerebellum, these SHH targets include *PTCH1*, *PTCH2*, *GLI1*, *N-MYC*, *CyclinD1*, *Bmi*, *Gpr153*, *Foxo6*, *YAP1*, *Neuropilin1* and *NCOR2* [81]. Recently, we identified *NEO1*, a death receptor for Netrin-1, as a gene controlled by the SHH/GLI pathway in SHH-driven MB [82].

To further investigate *NTN1* expression across MB groups, we performed a transcriptomic meta-analysis comparing expression levels in SHH-MB, WNT-MB, and normal cerebellum samples. This analysis revealed elevated *NTN1* expression in both SHH-MB and WNT-MB compared to other MB groups and normal tissue. We propose that *NTN1* overexpression in SHH-MB results from constitutive activation of the canonical SHH pathway, while overexpression of *NTN1* in the WNT-MB group likely involves other regulatory mechanisms [38, 54]. Recent studies have linked *NTN1* expression with WNT pathway activation, as demonstrated in various cellular contexts. Netrin-1 binding to *UNC5B* induces FAK-mediated inactivation of GSK3α/β in mouse embryonic stem cells, thereby stabilizing β-catenin [48]. Additionally, Boyé et al. showed that Netrin-1 interaction with *UNC5B* can activate Wnt/β-catenin signaling through LRP6 phosphorylation in endothelial cells, regulating blood-brain barrier integrity [83]. Subsequently, Furtado et al. demonstrated that Netrin-1 can regulate hematoretinal integrity through a similar mechanism, where Netrin-1 binding to *UNC5B* activates LRP5 phosphorylation and stabilizes β-catenin in endothelial cells [84]. Moreover, Xia et al. have recently shown that a Netrin-1/*UNC5B*-neogenin receptor axis can potentiate β-catenin expression, thereby amplifying Wnt signaling activity, in colorectal cancer [96]. These studies underscore the importance of studying Netrin-1 regulation and its diverse roles in both physiological and pathological contexts. Taken together, our results highlight prominent Netrin-1 expression in SHH-driven MB, with some expression also observed in WNT-subtype tumors, suggesting that its role outside the SHH context deserves future study.

It is important to note that all transcriptional and chromatin-based assays in this study were performed using DAOY cells. While acknowledging recent debates regarding the ontogeny of the DAOY line, we utilized it here as a well-characterized, SHH-responsive pediatric CNS model. Furthermore, its *TP53*-mutant status aligns with the SHH-activated *TP53*-mutant subtype defined by the WHO classification. While this genetic background may influence *GLI1*-mediated transcription and limit

the generalizability of our findings to all SHH subtypes, it provides a relevant model for this high-risk category. Future studies should validate these results in additional models, including those representing SHH-*TP53*-wild-type tumors.

On the other hand, while in vitro studies often identify transcription factor binding to consensus sites, not all sequences exhibit the same activity in vivo [85]. Our analysis revealed a functional GBS in an *NTN1* regulatory region, capable of transcriptional activation upon GLI induction, which aligns with in vivo data on *NTN1* expression during development and tumor progression. GBS elements in both promoters and enhancers can act in a tissue-specific manner, depending on local GLI effector concentrations [86]. This explains how SHH-dependent Netrin-1 expression can be dynamically regulated by the same genetic elements in different contexts. Interestingly, both in vitro and in vivo evidence links the SHH/GLI signaling pathway with Netrin-1 modulation in a wide variety of species. Hence, the conservation of SHH/GLI-Netrin-1 signaling mechanisms across species suggests a conserved regulatory framework.

Sequencing studies in MB cohorts have revealed differential distribution of chromatin state markers—such as H3K4me—across molecular groups, particularly in genes with key biological functions [87]. The dynamic interplay between repressive (H3K27me) and activating (H3K4me) histone modifications at regulatory elements of neural lineage genes is critical for maintaining the progenitor state [87, 88]. Disruption of this chromatin balance can trigger cell differentiation through activation of pro-differentiation transcriptional programs. In this context, the *NTN1* gene harbors putative intronic regulatory elements that are recognized by GLI transcription factors, suggesting a potential mechanism by which SHH/GLI signaling may regulate *NTN1* expression. Furthermore, these intronic GBSs exhibit transcriptionally active enhancer marks—such as H3K4me1 and H3K27ac [89]—which would support their role as enhancer elements responsive to SHH/GLI signaling.

In addition to GBSs in the regulatory regions of *NTN1*, we identified an E-box sequence located 171 bp downstream of the *GLI1*-responding GBS (Fig. 2B). E-box sequences are recognized by bHLH factors and recent studies suggest that the E-box/bHLH transcriptional factors cooperate with *GLI1* to regulate downstream SHH target genes during the transformation of GNPs to tumor cells (MB) [90–92]. One bHLH transcriptional factor strongly involved with cerebellum development is Atoh1, which controls cell-specification in the first rhombomere, the origin of the cerebellar neuronal population [93]. Notably, Atoh1 is essential for maintaining GNPs in an SHH-responsive state, inhibiting their differentiation [90–92]. Overexpression of Atoh1 in GNPs results in a significant increase in Netrin-1 expression (+ 2.16-fold change over the control) [90]. Furthermore, Atoh1 function is regulated downstream of Shh/Gli signaling [94], contributing to the up-regulation of Netrin-1 expression level in a Shh/GLI overactivated context. Atoh1 and *Gli1* cooperate in the transformation of GNPs to MB-initiating precursor cells, promoting aggressive tumor growth in murine models [90, 91]. Clinical data also correlate Netrin-1 and ATOH1 expression levels in human MB [90]. This evidence suggests that *GLI1* and ATOH1 may jointly regulate Netrin-1 transcription in MB, warranting further investigation.

The precise cell of origin for SHH MB remains debated. Given the heterogeneity within and between MB groups, several studies suggest the presence of subpopulations in SHH subtype MB, including CD15/SSEA1, stem cell-like CD133, and neural stem cell marker *SOX2*-enriched cell populations, pointing to a potential cancer stem/progenitor cell [72, 73]. Our data suggest the existence of a Netrin-1 positive tumor stem cell.

Netrin-1 has been established as a modulator of pluripotency in embryonic stem cells (ESCs), where it maintains cells in an undifferentiated, naïve state via *NEO1* and *UNC5B* receptor activation [48]. Consistent with this role in promoting stem-like phenotypes, Netrin-1 has been implicated in the stemness, relapse, and drug resistance of breast and ovarian cancers [52] and most recently, in driving sphere formation in colorectal cancer [95, 96]. Based on this landscape, we explored the role of Netrin-1 in MB. Using CRISPRi, we demonstrated that Netrin-1 is required for tumorsphere formation in the SHH-MB DAOY cell line. Furthermore, Netrin-1 knockdown significantly reduced expression of CD24, a validated marker of MB-initiating neural progenitor cells [74], confirming that Netrin-1 is critical for maintaining the progenitor pool in MB. Importantly, the persistence of Netrin-1 expression in these tumorsphere assays without exogenous SHH supplementation highlights that *NTN1* regulation in cancer is not strictly or exclusively dependent on the SHH pathway. While SHH is a known regulator, transcription in tumors is heavily influenced by alternative, SHH-independent mechanisms. For instance, NF-κB acts as a direct transcriptional activator of *NTN1* in various tumor and inflammatory contexts [54]. Additionally, stress-response pathways involving p53 and its isoform Δ40p53 directly bind the *NTN1* promoter to upregulate its expression and promote cell survival [97]. Furthermore, basal *NTN1* expression levels are strongly governed by chromatin context and epigenetic regulation, such as DNA methylation [98]. Together, these intersecting inflammatory, stress-responsive, and epigenetic pathways likely maintain the robust Netrin-1 expression required to support cancer stem cell self-renewal even in the absence of active SHH supplementation [99].

While our data demonstrate a robust functional impairment of CSC traits following Netrin-1 knockdown, we noted that supplementation with exogenous recombinant Netrin-1 was insufficient to rescue the phenotype. We postulate that this is due to the complex autocrine and intracrine dynamics of the Netrin-1 signaling axis. First, Netrin-1 and its dependence receptors (e.g., *NEO1*, *UNC5B*) are tightly co-regulated via transcriptional positive feedback loops [97]. Prolonged knockdown of endogenous Netrin-1 likely leads to the secondary downregulation of its surface receptors, rendering the cells deaf to extracellular recombinant ligands. Second, Netrin-1 exhibits critical intracrine activity; specifically, truncated intracellular isoforms (such as ΔN-Netrin-1) localize to the nucleolus to drive cell proliferation and stemness independent of surface receptor engagement [41, 42]. Because recombinant Netrin-1 cannot cross the cell membrane to restore these depleted intracellular pools, our findings suggest that the intracellular/nuclear localizations of Netrin-1 are functionally indispensable for maintaining the CSC phenotype in this model.

Mechanistically, our data suggest that Netrin-1 could regulate this stemness by suppressing downstream ERK signaling. This finding stands in sharp contrast to the recently published mechanism in adult colorectal cancer, where Netrin-1 was shown to activate ERK to drive proliferation [96]. However, our observation strongly resonates with the embryonic nature of pediatric malignancies, which frequently co-opt developmental programs to maintain a primitive phenotype. Our results mirror the mechanism described by Huyghe et al. [48] in ESCs, where Netrin-1 prevents differentiation by recruiting PP2A to dephosphorylate and inhibit ERK1/2. By dampening ERK activity, which acts as a pro-differentiation signal in this developmental context, Netrin-1 effectively enforces a 'differentiation block,' locking these pediatric cancer cells in a high-potency, stem-like state.

Importantly, pharmacological inhibition of Netrin-1 via NP137, a monoclonal antibody that blocks Netrin-1, prevents cancer progression by selectively targeting cancer stem cells. NP137 is currently in phase I clinical trials for various solid tumors [100].

These findings underscore the central role of SHH/GLI signaling in sustaining stemness-like phenotypes across different cancer contexts, with Netrin-1 acting as a key mediator. Depending on the receptor or combination of receptors activated downstream, Netrin-1 promotes both cell survival and stemness features in MB. Our previous work demonstrated that *NEO1* was highly expressed in SHH-driven MB [82]. However, the precise interaction between Netrin-1 and *NEO1* in SHH-driven MB requires further investigation.

In the clinical context, survival rates for MB patients have reached approximately 70–80% due to conventional treatments, including surgery, craniospinal radiotherapy (for children over 3 years old), and chemotherapy. While these advancements represent significant progress, many survivors experience long-term adverse effects, including developmental, neurological, neuroendocrine, and psychosocial complications [101]. One of the most detrimental side effects of radiotherapy is the profound impact on patients' cognitive development. This underscores the urgent need for molecular characterization of MB subgroups to facilitate the implementation of stratified, precision-guided therapies. Supporting this notion, a recent study showed that combining *SMO* inhibitors with anti–Netrin-1 produces a synergistic effect, effectively suppressing MB cell survival and tumor growth both in vitro and in vivo [102]. Our findings establish a mechanistic link between Netrin-1 and SHH-driven MB progression, GLI-dependent transcriptional activation of Netrin-1 sustains tumor cell self-renewal by engaging survival signaling pathways, thereby reinforcing the stem-like state and contributing to tumor persistence, which are important as a target in the context of personalized medicine.

Supplementary Information

The online version contains supplementary material available at https://doi.org/10.1186/s12964-026-02993-y.

Supplementary Material 1.

Supplementary Material 2.

Acknowledgements

We are grateful to Dr. James Briscoe laboratory for kindly sharing the GLI3 over-expressing and control constructs. We greatly appreciate Dr. Martin Montecino and lab members for their assistance with the Chip assays.

Authors' contributions

Author Contributions: P.F. and E.F-C. contributed equally to this work and are co-first authors. Conceptualization: V.P., P.F., and E.F-C. S.P. and M.K. performed the initial gene expression profiling studies. Experiments were performed by P.F., E.F-C., J.M.Z-H., C.P., B.G-R., F.A-A., and R.A., who also analyzed the data and assisted in figure preparation. B.W. contributed to manuscript revision and discussion of the results. V.P. and M.V-G. served as co-corresponding authors, reviewed the manuscript, and ensured the accuracy of the analyses. All authors read and approved the final manuscript.† These authors contributed equally to this work.

Funding

This work was supported by Fondecyt grants 1140697 and 1221522 (VP), 1230983 (MV-G), and 3200825 (FA-A); Centro Basal Ciencia & Vida, ANID FB210008 (MV-G); CONICYT doctoral grants 21120358 (PF), 21181605 (EF-C), and 21230341 (BG-R); and CONICYT International Internship and travel doctoral grants.

Data availability

The datasets generated and/or analyzed during the current study are available from the corresponding author on reasonable request.

Declarations

Ethics approval and consent to participate

Human samples used in this study were obtained from previously established biobanks with informed consent and appropriate ethical approval.

Competing interests

The authors declare no competing interests.

Author details

[1]Laboratory of Stem Cells and Developmental Biology, Faculty of Sciences, Universidad de Chile, Las Encinas 3370. Milenio Building Floor 3, Santiago, Ñuñoa 7800024, Chile
[2]Facultad de Ciencia, Universidad San Sebastián, Sede Concepción, Concepción, Chile
[3]Cancer Cell Biology Laboratory, Centro de Biología Celular y Biomedicina (CEBICEM), Facultad de Ciencia, Universidad San Sebastián, Santiago, Chile
[4]Hopp Children's Cancer Center Heidelberg (KiTZ), Heidelberg, Germany
[5]Division of Pediatric Neurooncology, German Cancer Consortium (DKTK), German Cancer Research Center (DKFZ), Heidelberg, Germany
[6]Department of Pediatric Hematology and Oncology, Heidelberg University Hospital and National Center for Tumor Diseases (NCT), Heidelberg, Germany
[7]Princess Máxima Center for Pediatric Oncology, Utrecht, the Netherlands
[8]University Medical Center Utrecht (UMCU), Utrecht, the Netherlands
[9]Department of Pediatric Hematology and Oncology, University Medical Center Hamburg-Eppendorf, Hamburg, Germany
[10]Research Institute Children's Cancer Center Hamburg, Hamburg, Germany
[11]Institute of Neuropathology, University Medical Center Hamburg-Eppendorf, Hamburg, Germany
[12]The University of Queensland Frazer Institute, Translational Research Institute, Woolloongabba, QLD, Australia
[13]Department of Pediatric Hematology and Oncology, University Medical Center of Saarland, Saarland University, Homburg, Germany
[14]Hematology-Oncology Section, Department of Pediatrics - Hematology/Oncology and Neurosurgery, Texas Children's Cancer Center, Baylor College of Medicine, Houston, TX, USA
[15]Centro de Genética y Genómica, Facultad de Medicina Clínica Alemana Universidad del Desarrollo, Santiago, Chile
[16]Centro Ciencia & Vida, Fundación Ciencia & Vida, Santiago, Chile

Received: 11 August 2025 / Accepted: 4 June 2026
Published online: 15 June 2026

References

1. Milenkovic L, Goodrich LV, Higgins KM, Scott MP. Mouse patched1 controls body size determination and limb patterning. Development. 1999;126(20):4431–40. https://doi.org/10.1242/dev.126.20. .4431 PubMed PMID: 10498679.
2. Ruiz i Altaba A, Palma V, Dahmane N. Hedgehog-Gli signalling and the growth of the brain. Nat Rev Neurosci. 2002;3(1):24–33. https://doi.org/10.1038/nrn704 . PubMed PMID: 11823802.
3. Ingham PW. Hedgehog signaling. Curr Top Dev Biol. 2022;149:1–58. https://doi.org/10.1016/bs.ctdb.2022.04. .003 PubMed PMID: 35606054.
4. Ingham PW, Nakano Y, Seger C. Mechanisms and functions of Hedgehog signalling across the metazoa. Nat Rev Genet. 2011;12(6):393–406. https://doi.org/10.1038/nrg2984 . PubMed PMID: 21502959.
5. Palma V, Ruiz i Altaba A. Hedgehog-GLI signaling regulates the behavior of cells with stem cell properties in the developing neocortex. Development. 2004;131(2):337–45. https://doi.org/10.1242/dev.00930 . PubMed PMID: 14681189.
6. Lewis PM, Gritli-Linde A, Smeyne R, Kottmann A, McMahon AP. Sonic hedgehog signaling is required for expansion of granule neuron precursors and patterning of the mouse cerebellum. Dev Biol. 2004;270(2):393–410. https://doi.org/10.1016/j.ydbio. 2004.03.007 PubMed PMID: 15183722.
7. Wechsler-Reya R, Scott MP. The developmental biology of brain tumors. Annu Rev Neurosci. 2001;24:385–428. https://doi.org/10.1146/annurev.neuro.24.1. .385 PubMed PMID: 11283316.
8. Rubin JB, Rowitch DH. Medulloblastoma: a problem of developmental biology. Cancer Cell. 2002;2(1):7–8. https://doi.org/10.1016/s1535-6108. (02)00090-9 PubMed PMID: 12150819.
9. Wechsler-Reya RJ, Scott MP. Control of neuronal precursor proliferation in the cerebellum by Sonic Hedgehog. Neuron. 1999;22(1):103–14. https://doi.org/10.1016/s0896-6273(. 00)80682-0 PubMed PMID: 10027293.
10. Wallace VA. Purkinje-cell-derived Sonic hedgehog regulates granule neuron precursor cell proliferation in the developing mouse cerebellum. Curr Biol. 1999;9(8):445–8. https://doi.org/10.1016/s0960-9822. (99)80195-x PubMed PMID: 10226030.
11. Dahmane N, Ruiz i Altaba A. Sonic hedgehog regulates the growth and patterning of the cerebellum. Development. 1999;126(14):3089–100. https://doi.org/10.1242/dev.126. .14.3089 PubMed PMID: 10375501.
12. Gajjar AJ, Robinson GW. Medulloblastoma-translating discoveries from the bench to the bedside. Nat Rev Clin Oncol. 2014;11(12):714–22. https://doi.org/10.1038/nrclinonc.2014.181 . PubMed PMID: 25348790.
13. Goodrich LV, Milenković L, Higgins KM, Scott MP. Altered neural cell fates and medulloblastoma in mouse patched mutants. Science. 1997;277(5329):1109–13. https://doi.org/10.1126/science.277.5329. .1109 PubMed PMID: 9262482.
14. Northcott PA, Hielscher T, Dubuc A, Mack S, Shih D, Remke M, et al. Pediatric and adult sonic hedgehog medulloblastomas are clinically and molecularly distinct. Acta Neuropathol. 2011;122(2):231–40. https://doi.org/10.1007/s00401-011-0846-7 . PubMed PMID: 21681522.
15. Millard NE, De Braganca KC, Medulloblastoma. J Child Neurol. 2016;31(12):1341–53. doi:10.1177/0883073815600866 PubMed PMID: 26336203.
16. Ellison DW. Childhood medulloblastoma: novel approaches to the classification of a heterogeneous disease. Acta Neuropathol. 2010;120(3):305–16. https://doi.org/10.1007/s00401-010-0726-6 . PubMed PMID: 20652577.
17. Yao E, Chuang PT. Hedgehog signaling: From basic research to clinical applications. J Formos Med Assoc. 2015;114(7):569–76. https://doi.org/10.1016/j.jfma.2015.01. .005 PubMed PMID: 25701396.
18. Winklmayr M, Schmid C, Laner-Plamberger S, Kaser A, Aberger F, Eichberger T, et al. Non-consensus GLI binding sites in Hedgehog target gene regulation. BMC Mol Biol. 2010;11:2. https://doi.org/10.1186/1471-2199-11-2 . PubMed PMID: 20070907.
19. Aberger F, Ruiz i Altaba A. Context-dependent signal integration by the GLI code: the oncogenic load, pathways, modifiers and implications for cancer therapy. Semin Cell Dev Biol. 2014;33(100):93–104. https://doi.org/10.1016/j.semcdb.2014.05.003 . PubMed PMID: 24852887.
20. Lee EY, Ji H, Ouyang Z, Zhou B, Ma W, Vokes SA, et al. Hedgehog pathway-regulated gene networks in cerebellum development and tumorigenesis. Proc Natl Acad Sci U S A. 2010;107(21):9736–41. https://doi.org/10.1073/pnas.1004602107 . PubMed PMID: 20460306.
21. Yamagishi S, Bando Y, Sato K. Involvement of Netrins and Their Receptors in Neuronal Migration in the Cerebral Cortex. Front Cell Dev Biol. 2020;8:590009. https://doi.org/10.3389/fcell.2020.590009 . PubMed PMID: 33520982.
22. Hedgecock EM, Culotti JG, Hall DH. The unc-5, unc-6, and unc-40 genes guide circumferential migrations of pioneer axons and mesodermal cells on the epidermis in C. elegans. Neuron. 1990;4(1):61–85. https://doi.org/10.1016/0896-6273. (90)90444-k PubMed PMID: 2310575.
23. Serafini T, Kennedy TE, Galko MJ, Mirzayan C, Jessell TM, Tessier-Lavigne M. The netrins define a family of axon outgrowth-promoting proteins homologous to C. elegans UNC-6. Cell. 1994;78(3):409–24. https://doi.org/10.1016/0092-8674. (94)90420-0 PubMed PMID: 8062384.
24. Serafini T, Colamarino SA, Leonardo ED, Wang H, Beddington R, Skarnes WC, et al. Netrin-1 is required for commissural axon guidance in the developing vertebrate nervous system. Cell. 1996;87(6):1001–14. https://doi.org/10.1016/s0092-8674. (00)81795-x PubMed PMID: 8978605.
25. Kennedy TE, Serafini T, de la Torre JR, Tessier-Lavigne M. Netrins are diffusible chemotropic factors for commissural axons in the embryonic spinal cord. Cell. 1994;78(3):425–35. https://doi.org/10.1016/0092-8674. (94)90421-9 PubMed PMID: 8062385.
26. Delloye-Bourgeois C, Fitamant J, Paradisi A, Cappellen D, Douc-Rasy S, Raquin MA, et al. Netrin-1 acts as a survival factor for aggressive Neuroblastoma. J Exp Med. 2009;206(4):833–47. 10. 1084/JEM.20082299, PubMed PMID: 19349462.
27. Llambi F, Causeret F, Bloch-Gallego E, Mehlen P. Netrin-1 acts as a survival factor via its receptors UNC5H and DCC. EMBO J. 2001;20(11):2715–22. https://doi.org/10.1093/emboj/20.11.2715 . PubMed PMID: 11387206.
28. Wilson BD, Ii M, Park KW, Suli A, Sorensen LK, Larrieu-Lahargue F, et al. Netrins promote developmental and therapeutic angiogenesis. Science.

2006;313(5787):640–4. https://doi.org/10.1126/science.1124704 . PubMed PMID: 16809490.
29. Yebra M, Montgomery AMP, Diaferia GR, Kaido T, Silletti S, Perez B, et al. Recognition of the neural chemoattractant Netrin-1 by integrins alpha6beta4 and alpha3beta1 regulates epithelial cell adhesion and migration. Dev Cell. 2003;5(5):695–707. https://doi.org/10.1016/s1534-5807. (03)00330-7 PubMed PMID: 14602071.
30. Ly NP, Komatsuzaki K, Fraser IP, Tseng AA, Prodhan P, Moore KJ, et al. Netrin-1 inhibits leukocyte migration in vitro and in vivo. Proc Natl Acad Sci U S A. 2005;102(41):14729–34. https://doi.org/10.1073/pnas.0506233102 . PubMed PMID: 16203981.
31. Tadagavadi RK, Wang W, Ramesh G. Netrin-1 regulates Th1/Th2/Th17 cytokine production and inflammation through *UNC5B* receptor and protects kidney against ischemia-reperfusion injury. J Immunol. 2010;185(6):3750–8. https://doi.org/10.4049/jimmunol.1000435. PubMed PMID: 20693423.
32. Chen Z, Chen Y, Zhou J, Li Y, Gong C, Wang X. Netrin-1 reduces lung ischemia-reperfusion injury by increasing the proportion of regulatory T cells. J Int Med Res. 2020;48(6):300060520926415. doi:10.1177/0300060520926415 PubMed PMID: 32485133.
33. Cynn E, Li DY, O'Reilly ME, Wang Y, Bashore AC, Jha A, et al. Human Macrophage Long Intergenic Noncoding RNA, SIMALR, Suppresses Inflammatory Macrophage Apoptosis via *NTN1* (Netrin-1). Arterioscler Thromb Vasc Biol. 2023;43(2):286–99. https://doi.org/10.1161/ATVBAHA.122.318353 . PubMed PMID: 36546321.
34. Ylivinkka I, Sihto H, Tynninen O, Hu Y, Laakso A, Kivisaari R, et al. Motility of glioblastoma cells is driven by netrin-1 induced gain of stemness. J Exp Clin Cancer Res. 2017;36(1):9. https://doi.org/10.1186/s13046-016-0482-0 . PubMed PMID: 28069038.
35. Akino T, Han X, Nakayama H, McNeish B, Zurakowski D, Mammoto A, et al. Netrin-1 promotes medulloblastoma cell invasiveness and angiogenesis, and demonstrates elevated expression in tumor tissue and urine of patients with pediatric medulloblastoma. Cancer Res. 2014;74(14):3716–26. https://doi.org/10.1158/0008-5472.CAN-13-3116 . PubMed PMID: 24812271.
36. Wischhusen J, Wilson KE, Delcros JG, Molina-Peña R, Gibert B, Jiang S, et al. Ultrasound molecular imaging as a non-invasive companion diagnostic for netrin-1 interference therapy in breast cancer. Theranostics. 2018;8(18):5126–42. https://doi.org/10.7150/thno.27221 . PubMed PMID: 30429890.
37. Yin K, Wang L, Zhang X, He Z, Xia Y, Xu J, et al. Netrin-1 promotes gastric cancer cell proliferation and invasion via the receptor neogenin through PI3K/AKT signaling pathway. Oncotarget. 2017;8(31):51177–89. https://doi.org/10.18632/oncotarget.17750 . PubMed PMID: 28881639.
38. Arakawa H. Netrin-1 and its receptors in tumorigenesis. Nat Rev Cancer. 2004;4(12):978–87. https://doi.org/10.1038/nrc. 1504 PubMed PMID: 15573119.
39. Dumartin L, Quemener C, Laklai H, Herbert J, Bicknell R, Bousquet C, Pyronnet S, Castronovo V, Schilling MK, Bikfalvi A, Hagedorn M. Netrin-1 mediates early events in pancreatic adenocarcinoma progression, acting on tumor and endothelial cells. Gastroenterology. 2010;138(4):1595-606, 1606.e1-8. https://doi.org/10.1053/j.gastro.2009.12.061. Epub 2010 Jan 18. PMID: 20080097.
40. Yin K, Wang L, Xia Y, Dang S, Zhang X, He Z, et al. Netrin-1 promotes cell neural invasion in gastric cancer via its receptor neogenin. J Cancer. 2019;10(14):3197–207. https://doi.org/10.7150/jca.30230 . PubMed PMID: 31289590.
41. Delloye-Bourgeois C, Goldschneider D, Paradisi A, Therizols G, Belin S, Hacot S, et al. Nucleolar localization of a netrin-1 isoform enhances tumor cell proliferation. Sci Signal. 2012;5(236):ra57. https://doi.org/10.1126/scisignal.2002456 . PubMed PMID: 22871610.
42. Harter PN, Zinke J, Scholz A, Tichy J, Zachskorn C, Kvasnicka HM, et al. Netrin-1 expression is an independent prognostic factor for poor patient survival in brain metastases. PLoS ONE. 2014;9(3):e92311. https://doi.org/10.1371/journal.pone.0092311 . PubMed PMID: 24647424.
43. Link BC, Reichelt U, Schreiber M, Kaifi JT, Wachowiak R, Bogoevski D, et al. Prognostic implications of netrin-1 expression and its receptors in patients with adenocarcinoma of the pancreas. Ann Surg Oncol. 2007;14(9):2591–9. https://doi.org/10.1245/s10434-007-9469-6 . PubMed PMID: 17549567.
44. Papanastasiou AD, Pampalakis G, Katsaros D, Sotiropoulou G. Netrin-1 overexpression is predictive of ovarian malignancies. Oncotarget. 2011;2(5):363–7. https://doi.org/10.18632/oncotarget.258 . PubMed PMID: 21789787.
45. Ramesh G, Berg A, Jayakumar C. Plasma netrin-1 is a diagnostic biomarker of human cancers. Biomarkers. 2011;16(2):172-80. https://doi.org/10.3109/1354750X.2010.541564. Epub 2011 Feb 8. PMID: 21303223; PMCID: PMC3143477.
46. Kefeli U, Yildirim ME, Aydin D, Madenci OC, Yasar N, Sener N, Mert AG, Yuksel S, Ercelep OB, Korkmaz T, Yildiz R, Gumus M. Netrin-1 concentrations in patients with advanced gastric cancer and its relation with treatment. Biomarkers. 2012;17(7):663-7. https://doi.org/10.3109/1354750X.2012.709882. Epub 2012 Aug 13. PMID: 22889408.
47. Perampalam P, MacDonald JI, Zakirova K, Passos DT, Wasif S, Ramos-Valdes Y, et al. Netrin signaling mediates survival of dormant epithelial ovarian cancer cells. Elife. 2024;12. 10. 7554/eLife.91766 PubMed PMID: 39023520.
48. Huyghe A, Furlan G, Ozmadenci D, Galonska C, Charlton J, Gaume X, et al. Netrin-1 promotes naive pluripotency through Neo1 and *UNC5B* co-regulation of Wnt and MAPK signalling. Nat Cell Biol. 2020;22(4):389–400. https://doi.org/10.1038/s41556-020-0483-2. PubMed PMID: 32231305.
49. Sung PJ, Rama N, Imbach J, Fiore S, Ducarouge B, Neves D, et al. Cancer-Associated Fibroblasts Produce Netrin-1 to Control Cancer Cell Plasticity. Cancer Res. 2019;79(14):3651–61. https://doi.org/10.1158/0008-5472.CAN-18-2952 . PubMed PMID: 31088838.
50. Renders S, Svendsen AF, Panten J, Rama N, Maryanovich M, Sommerkamp P, et al. Niche derived netrin-1 regulates hematopoietic stem cell dormancy via its receptor neogenin-1. Nat Commun. 2021;12(1):608. https://doi.org/10.1038/s41467-020-20801-0 . PubMed PMID: 33504783.
51. Sanvoranart T, Supokawej A, Kheolamai P, U-Pratya Y, Poungvarin N, Sathornsumetee S, et al. Targeting Netrin-1 in glioblastoma stem-like cells inhibits growth, invasion, and angiogenesis. Tumour Biol. 2016;37(11):14949–60. https://doi.org/10.1007/s13277-016-5314-5 . PubMed PMID: 27651158.
52. Ducarouge B, Redavid AR, Victoor C, Chira R, Fonseca A, Hervieu M, et al. Netrin-1 blockade inhibits tumor associated Myeloid-derived suppressor cells, cancer stemness and alleviates resistance to chemotherapy and immune checkpoint inhibitor. Cell Death Differ. 2023;30(10):2201-12. https://doi.org/10.1038/s41418-023-01209-x. Epub 2023 Aug 26. PMID: 37633969; PMCID: PMC10589209.
53. Wang Z, Zhang H, Xu S, Liu Z, Cheng Q. The adaptive transition of glioblastoma stem cells and its implications on treatments. Signal Transduct Target Ther. 2021;6(1):124. https://doi.org/10.1038/s41392-021-00491-w. PMID: 33753720; PMCID: PMC7985200.
54. Paradisi A, Maisse C, Bernet A, Coissieux MM, Maccarrone M, Scoazec JY, et al. NF-kappaB regulates netrin-1 expression and affects the conditional tumor suppressive activity of the netrin-1 receptors. Gastroenterology. 2008;135(4):1248–57. https://doi.org/10.1053/j.gastro. .2008.06.080 PubMed PMID: 18692059.
55. Charron F, Stein E, Jeong J, McMahon AP, Tessier-Lavigne M. The morphogen sonic hedgehog is an axonal chemoattractant that collaborates with netrin-1 in midline axon guidance. Cell. 2003;113(1):11–23. https://doi.org/10.1016/s0092-8674. (03)00199-5 PubMed PMID: 12679031.
56. Watanabe K, Tamamaki N, Furuta T, Ackerman SL, Ikenaka K, Ono K. Dorsally derived netrin 1 provides an inhibitory cue and elaborates the waiting period for primary sensory axons in the developing spinal cord. Development. 2006;133(7):1379–87. https://doi.org/10.1242/dev.02312 . PubMed PMID: 16510500.
57. Hakanen J, Duprat S, Salminen M. Netrin1 is required for neural and glial precursor migrations into the olfactory bulb. Dev Biol. 2011;355(1):101–14. https://doi.org/10.1016/j.ydbio.2011. 04.016 PubMed PMID: 21545793.
58. Guijarro P, Simó S, Pascual M, Abasolo I, Del Río JA, Soriano E. Netrin1 exerts a chemorepulsive effect on migrating cerebellar interneurons in a Dcc-independent way. Mol Cell Neurosci. 2006;33(4):389–400. 08.010 PubMed PMID: 17029983.
59. Bergeron SA, Milla LA, Villegas R, Shen MC, Burgess SM, Allende ML, et al. Expression profiling identifies novel Hh/Gli-regulated genes in developing zebrafish embryos. Genomics. 2008;91(2):165–77. https://doi.org/10.1016/j.ygeno.2007.09.001 . PubMed PMID: 18055165.
60. Xu J, Srinivas BP, Tay SY, Mak A, Yu X, Lee SGP, et al. Genomewide expression profiling in the zebrafish embryo identifies target genes regulated by Hedgehog signaling during vertebrate development. Genetics. 2006;174(2):735–52. https://doi.org/10.1534/genetics.106.061523 . PubMed PMID: 16888327.
61. Podjaski C, Alvarez JI, Bourbonniere L, Larouche S, Terouz S, Bin JM, et al. Netrin 1 regulates blood-brain barrier function and neuroinflammation. Brain. 2015;138(Pt 6):1598–612. https://doi.org/10.1093/brain/awv092 . PubMed PMID: 25903786.
62. Weishaupt H, Johansson P, Sundström A, Lubovac-Pilav Z, Olsson B, Nelander S, et al. Batch-normalization of cerebellar and medulloblastoma gene expression datasets utilizing empirically defined negative control genes. Bioinformatics. 2019;35(18):3357–64. https://doi.org/10.1093/bioinformatics/btz066 . PubMed PMID: 30715209.

63. Grant CE, Bailey TL, Noble WS. FIMO: scanning for occurrences of a given motif. Bioinformatics. 2011;27(7):1017–8. https://doi.org/10.1093/bioinformatics/btr064 . PubMed PMID: 21330290.
64. Shim KW, Joo SY, Kim SH, Choi JU, Kim DS. Prediction of prognosis in children with medulloblastoma by using immunohistochemical analysis and tissue microarray. J Neurosurg Pediatr. 2008;1(3):196–205. https://doi.org/10.3171/PED/2008/1/3/196 . PubMed PMID: 18352763.
65. Sasaki H, Hui C, Nakafuku M, Kondoh H. A binding site for Gli proteins is essential for HNF-3beta floor plate enhancer activity in transgenics and can respond to Shh in vitro. Development. 1997;124(7):1313–22. https://doi.org/10.1242/dev.124.7.1313 . PubMed PMID: 9118802.
66. Sena-Esteves M, Tebbets JC, Steffens S, Crombleholme T, Flake AW. Optimized large-scale production of high titer lentivirus vector pseudotypes. J Virol Methods. 2004;122(2):131–9. 08.017 PubMed PMID: 15542136.
67. Bhagwat SV, McMillen WT, Cai S, Zhao B, Whitesell M, Shen W, et al. ERK Inhibitor LY3214996 Targets ERK Pathway-Driven Cancers: A Therapeutic Approach Toward Precision Medicine. Mol Cancer Ther. 2020;19(2):325–36. https://doi.org/10.1158/1535-7163.MCT-19-0183 . PubMed PMID: 31744895.
68. Northcott PA, Korshunov A, Witt H, Hielscher T, Eberhart CG, Mack S, et al. Medulloblastoma comprises four distinct molecular variants. J Clin Oncol. 2011;29(11):1408–14. https://doi.org/10.1200/JCO. 2009.27.4324 PubMed PMID: 20823417.
69. Orr BA. Pathology, diagnostics, and classification of medulloblastoma. Brain Pathol. 2020;30(3):664–78. https://doi.org/10.1111/bpa.12837 . PubMed PMID: 32239782.
70. Cotter JA, Hawkins C, Medulloblastoma. WHO 2021 and Beyond. Pediatr Dev Pathol. 2022;25(1):23–33. doi:10.1177/10935266211018931 PubMed PMID: 35168417.
71. Soutoglou E, Talianidis I. Coordination of PIC assembly and chromatin remodeling during differentiation-induced gene activation. Science. 2002;295(5561):1901–4. https://doi.org/10.1126/science.1068356 . PubMed PMID: 11884757.
72. Takanaga H, Tsuchida-Straeten N, Nishide K, Watanabe A, Aburatani H, Kondo T. Gli2 is a novel regulator of sox2 expression in telencephalic neuroepithelial cells. Stem Cells. 2009;27(1):165–74. https://doi.org/10.1634/stemcells.2008-0580 . PubMed PMID: 18927476.
73. Ahlfeld J, Favaro R, Pagella P, Kretzschmar HA, Nicolis S, Schüller U. Sox2 requirement in sonic hedgehog-associated medulloblastoma. Cancer Res. 2013;73(12):3796–807. https://doi.org/10.1158/0008-5472.CAN-13-0238 . PubMed PMID: 23596255.
74. Robson JP, Remke M, Kool M, Julian E, Korshunov A, Pfister SM, et al. Identification of CD24 as a marker of Patched1 deleted medulloblastoma-initiating neural progenitor cells. PLoS ONE. 2019;14(1):e0210665. https://doi.org/10.1371/journal.pone.0210665 . PubMed PMID: 30657775.
75. Mehlen P, Thibert C. Dependence receptors: between life and death. Cell Mol Life Sci. 2004;61(15):1854–66. https://doi.org/10.1007/s00018-004-3467-7 . PubMed PMID: 15289929.
76. Sasaki H, Nishizaki Y, Hui C, Nakafuku M, Kondoh H. Regulation of Gli2 and Gli3 activities by an amino-terminal repression domain: implication of Gli2 and Gli3 as primary mediators of Shh signaling. Development. 1999;126(17):3915–24. https://doi.org/10.1242/dev.126.17.3915 . PubMed PMID: 10433919.
77. Northcott PA, Jones DTW, Kool M, Robinson GW, Gilbertson RJ, Cho YJ, et al. Medulloblastomics: the end of the beginning. Nat Rev Cancer. 2012;12(12):818–34. https://doi.org/10.1038/nrc3410 . PubMed PMID: 23175120.
78. Ramaswamy V, Remke M, Bouffet E, Bailey S, Clifford SC, Doz F, et al. Risk stratification of childhood medulloblastoma in the molecular era: the current consensus. Acta Neuropathol. 2016;131(6):821–31. https://doi.org/10.1007/s00401-016-1569-6 . PubMed PMID: 27040285.
79. Northcott PA, Shih DJH, Peacock J, Garzia L, Morrissy AS, Zichner T, et al. Subgroup-specific structural variation across 1,000 medulloblastoma genomes. Nature. 2012;488(7409):49–56. https://doi.org/10.1038/nature11327 . PubMed PMID: 22832581.
80. Yu M, Gipp J, Yoon JW, Iannaccone P, Walterhouse D, Bushman W. Sonic hedgehog-responsive genes in the fetal prostate. J Biol Chem. 2009;284(9):5620–9. https://doi.org/10.1074/jbc. .M809172200 PubMed PMID: 19095649.
81. Varnat F, Duquet A, Malerba M, Zbinden M, Mas C, Gervaz P, et al. Human colon cancer epithelial cells harbour active HEDGEHOG-GLI signalling that is essential for tumour growth, recurrence, metastasis and stem cell survival and expansion. EMBO Mol Med. 2009;1(6–7):338–51. https://doi.org/10.1002/emmm.200900039 . PubMed PMID: 20049737.
82. Milla LA, Arros A, Espinoza N, Remke M, Kool M, Taylor MD, et al. Neogenin1 is a Sonic Hedgehog target in medulloblastoma and is necessary for cell cycle progression. Int J Cancer. 2014;134(1):21–31. https://doi.org/10.1002/ijc.28330 . PubMed PMID: 23775842.
83. Boyé K, Geraldo LH, Furtado J, Pibouin-Fragner L, Poulet M, Kim D, et al. Endothelial *UNC5B* controls blood-brain barrier integrity. Nat Commun. 2022;13(1):1169. https://doi.org/10.1038/s41467-022-28785-9. PubMed PMID: 35246514.
84. Furtado J, Geraldo LH, Leser FS, Poulet M, Park H, Pibouin-Fragner L et al. Netrin-1 binding to *UNC5B* regulates Blood-Retina Barrier integrity. bioRxiv. 2023 Jan. https://doi.org/10.1101/2023.01.21.525006 PubMed PMID: 36711611.
85. Liu X, Lee CK, Granek JA, Clarke ND, Lieb JD. Whole-genome comparison of Leu3 binding in vitro and in vivo reveals the importance of nucleosome occupancy in target site selection. Genome Res. 2006;16(12):1517–28. https://doi.org/10.1101/gr.5655606 . PubMed PMID: 17053089.
86. Vokes SA, Ji H, McCuine S, Tenzen T, Giles S, Zhong S, et al. Genomic characterization of Gli-activator targets in sonic hedgehog-mediated neural patterning. Development. 2007;134(10):1977–89. https://doi.org/10.1242/dev.001966 . PubMed PMID: 17442700.
87. Dubuc AM, Remke M, Korshunov A, Northcott PA, Zhan SH, Mendez-Lago M, et al. Aberrant patterns of H3K4 and H3K27 histone lysine methylation occur across subgroups in medulloblastoma. Acta Neuropathol. 2013;125(3):373–84. https://doi.org/10.1007/s00401-012-1070-9 . PubMed PMID: 23184418.
88. Schuettengruber B, Martinez AM, Iovino N, Cavalli G. Trithorax group proteins: switching genes on and keeping them active. Nat Rev Mol Cell Biol. 2011;12(12):799–814. https://doi.org/10.1038/nrm3230 . PubMed PMID: 22108599.
89. Kimura H. Histone modifications for human epigenome analysis. J Hum Genet. 2013;58(7):439–45. https://doi.org/10.1038/jhg. 2013.66 PubMed PMID: 23739122.
90. Ayrault O, Zhao H, Zindy F, Qu C, Sherr CJ, Roussel MF. Atoh1 inhibits neuronal differentiation and collaborates with *Gli1* to generate medulloblastoma-initiating cells. Cancer Res. 2010;70(13):5618–27. https://doi.org/10.1158/0008-5472.CAN-09-3740. PubMed PMID: 20516124.
91. Chang CH, Zanini M, Shirvani H, Cheng JS, Yu H, Feng CH, et al. Atoh1 Controls Primary Cilia Formation to Allow for SHH-Triggered Granule Neuron Progenitor Proliferation. Dev Cell. 2019;48(2):184–e1995. https://doi.org/10.1016/j.devcel.2018.12.017 . PubMed PMID: 30695697.
92. Grausam KB, Dooyema SDR, Bihannic L, Premathilake H, Morrissy AS, Forget A, et al. ATOH1 Promotes Leptomeningeal Dissemination and Metastasis of Sonic Hedgehog Subgroup Medulloblastomas. Cancer Res. 2017;77(14):3766–77. https://doi.org/10.1158/0008-5472.CAN-16-1836 . PubMed PMID: 28490517.
93. Green MJ, Myat AM, Emmenegger BA, Wechsler-Reya RJ, Wilson LJ, Wingate RJT. Independently specified Atoh1 domains define novel developmental compartments in rhombomere 1. Development. 2014;141(2):389–98. https://doi.org/10.1242/dev.099119 . PubMed PMID: 24381197.
94. Forget A, Bihannic L, Cigna SM, Lefevre C, Remke M, Barnat M, et al. Shh signaling protects Atoh1 from degradation mediated by the E3 ubiquitin ligase Huwe1 in neural precursors. Dev Cell. 2014;29(6):649–61. https://doi.org/10.1016/j.devcel.2014.05.014 . PubMed PMID: 24960692.
95. Vercauteren Drubbel A, Pirard S, Kin S, Dassy B, Lefort A, Libert F, et al. Reactivation of the Hedgehog pathway in esophageal progenitors turns on an embryonic-like program to initiate columnar metaplasia. Cell Stem Cell. 2021;28(8):1411–e14277. https://doi.org/10.1016/j.stem. .2021.03.019 PubMed PMID: 33882290.
96. Xia X, Mao Z, Wang W, Zhao L, Xu M, Ma J, et al. Netrin-1-*UNC5B*/neogenin axis enhances the stemness of colorectal cancer cells. Cell Commun Signal. 2025;23(1):496. https://doi.org/10.1186/s12964-025-02489-1. PubMed PMID: 41233873.
97. Sun Y, Manceau A, Frydman L, Cappuccio L, Neves D, Basso V, et al. Δ40p53 isoform up-regulates netrin-1/*UNC5B* expression and potentiates netrin-1 pro-oncogenic activity. Proc Natl Acad Sci U S A. 2021;118(36). https://doi.org/10.1073/pnas.2103319118. PubMed PMID: 34470826.
98. Grandin M, Mathot P, Devailly G, Bidet Y, Ghantous A, Favrot C, et al. Inhibition of DNA methylation promotes breast tumor sensitivity to netrin-1 interference. EMBO Mol Med. 2016;8(8):863–77. https://doi.org/10.15252/emmm.201505945 . PubMed PMID: 27378792.

99. Luan F, Cui Y, Huang R, Yang Z, Qiao S. Comprehensive pan-cancer analysis reveals *NTN1* as an immune infiltrate risk factor and its potential prognostic value in SKCM. Sci Rep. 2025;15(1):3223. https://doi.org/10.1038/s41598-025-85444-x . PubMed PMID: 39863609.
100. Lengrand J, Pastushenko I, Vanuytven S, Song Y, Venet D, Sarate RM, et al. Pharmacological targeting of netrin-1 inhibits EMT in cancer. Nature. 2023;620(7973):402–8. https://doi.org/10.1038/s41586-023-06372-2 . PubMed PMID: 37532929.
101. Taylor MD, Northcott PA, Korshunov A, Remke M, Cho YJ, Clifford SC, et al. Molecular subgroups of medulloblastoma: the current consensus. Acta Neuropathol. 2012;123(4):465–72. https://doi.org/10.1007/s00401-011-0922-z . PubMed PMID: 22134537.
102. Talbot J, Fombonne J, Torrejon J, Babcock BR, McSwain LF, Rama N, et al. Sonic hedgehog medulloblastomas are dependent on Netrin-1 for survival. Nat Commun. 2025;16(1):5137. https://doi.org/10.1038/s41467-025-59612-6 . PubMed PMID: 40461501.

Publisher's note

Springer Nature remains neutral with regard to jurisdictional claims in published maps and institutional affiliations.